Sensors and Materials, Vol. 38, No. 10 (2026) 6241–6252
MYU Tokyo

S & M 4678

Applications of Nickel–iron Layered Double Hydroxides with Different Ni:Fe Ratios for CO_2 Adsorption and Alkaline Water Electrolysis

Wei-Ting Chuang,[1] Chih-Chia Wang,[2] Guan-Yu Chen,[1] and Shih-Chen Shi[1*]

[1]Department of Mechanical Engineering, National Cheng Kung University (NCKU), No. 1, University Road, Tainan 70101, Taiwan
[2]Department of Electrical and Electronic Engineering, Chung Cheng Institute of Technology, National Defense University, Taoyuan 335009, Taiwan

(Received July 1, 2026; accepted August 21, 2026)

Keywords: Ni–Fe layered double hydroxides, CO_2 capture, alkaline water electrolysis, green hydrogen, TEPA functionalization

To mitigate the global climate crisis and address the growing demand for environmental monitoring, in this study, we developed Ni–Fe layered double hydroxides (LDHs) with molar ratios of 2:1, 2.5:1, and 3:1 as a multifunctional platform for CO_2 capture, green hydrogen production, and advanced sensing applications. Characterization analysis confirmed the formation of ordered 2D nanosheets with an average size of ~300 nm, providing an optimal high-surface-area matrix for both catalytic and sensing interfaces. For carbon capture, the Ni–Fe LDH with a Ni:Fe molar ratio of 2:1 functionalized with 20 wt% tetraethylenepentamine achieved a peak uptake of 0.389 g CO_2/g, significantly outperforming other compositions owing to Fe^{3+}-enhanced Lewis acidity and hydroxyl density. Crucially, this extraordinary capture capacity translates into a massive mass-loading response, demonstrating its immense potential as an ultrasensitive recognition layer for gravimetric CO_2 gas sensors. Regarding electrolysis, the Ni–Fe LDH-coated nickel foam with a Ni:Fe molar ratio of 2:1 yielded 50 mL of H_2 over 15 h, representing an 11% improvement over bare nickel foam. Furthermore, this architecture maintained the lowest charge-transfer resistance (Rct), making it a highly promising conductive substrate for future electrochemical sensing. These results prove the 2:1 Ni:Fe ratio to be the optimal configuration for integrated carbon mitigation, clean energy production, and environmental monitoring technologies.

1. Introduction

The escalating global climate crisis, driven by unprecedented levels of anthropogenic CO_2 emissions, has catalyzed a rapid shift toward carbon capture, utilization, and storage (CCUS) technologies and toward a hydrogen-based economy.(1) Green hydrogen, produced via alkaline water electrolysis, is widely regarded as the most promising clean energy carrier.(2) However, the

*Corresponding author: e-mail: scshi@mail.ncku.edu.tw
https://doi.org/10.18494/SAM6505

ISSN 0914-4935 © MYU K.K.
https://myukk.org/

commercial viability of these green technologies remains constrained by material efficiency and the high cost of specialized catalysts. Developing multifunctional, earth-abundant materials that can simultaneously address carbon mitigation and clean fuel production is now a critical priority for the global energy market.

Despite recent progress, significant bottlenecks persist in both fields. In carbon capture, conventional solid adsorbents often face a trade-off between active-site density and pore accessibility, resulting in suboptimal adsorption capacity.[3,4] Furthermore, many amine-functionalized materials exhibit poor thermal stability or ineffective anchoring of active molecules.[5] Similarly, in alkaline water electrolysis, while bare nickel foam (NF) is a common conductive substrate, it is highly susceptible to surface corrosion and passivation in harsh alkaline environments, leading to rapid performance degradation and high charge-transfer resistance.[6,7] Most high-performance catalysts rely on noble metals suah as Pt and Ir, which are too expensive for large-scale industrial deployment.[8,9] Recent studies have further demonstrated that advanced nanostructured electrodes can significantly improve electrochemical performance while enabling real-time monitoring through electrochemical impedance spectroscopy (EIS). For example, Deng *et al.* reported that Ni–Fe layered double hydroxides (LDHs) grown on NF provided excellent electrocatalytic activity together with impedance-based performance monitoring during water splitting, highlighting the potential of multifunctional LDH architectures in integrated energy conversion and sensing applications.[10] These findings further emphasize that simultaneously optimizing surface chemistry, electron transport, and structural stability is essential for developing next-generation multifunctional materials. Crucially, fundamental material limitations, such as inadequate active-site accessibility, poor structural stability, and sluggish electron-transfer kinetics, still form a major research gap preventing the realization of highly responsive, integrated energy and sensing systems.

Besides electrocatalytic activity, recent studies have shown that the rational incorporation of bio-derived or nanoscale functional fillers can markedly enhance the structural robustness and surface functionality of polymeric materials. For instance, poly(vinyl alcohol)/Uncaria gambir composites exhibit improved tribological performance and environmental compatibility, demonstrating the effectiveness of natural additives in strengthening multifunctional material systems.[11] Similarly, hydroxypropyl methylcellulose composites reinforced with nanosized metallic and oxide additives exhibit superior load-bearing capability and enhanced tribological performance owing to strengthened interfacial interactions.[12]

These studies collectively demonstrate that nanoscale engineering is an effective strategy for tailoring the physicochemical properties of multifunctional materials, providing useful insights for designing LDH-based hybrid systems for energy and sensing applications. In this study, we propose Ni–Fe LDHs as a dual-functional platform for CO_2 capture and green hydrogen production.[13,14] We hypothesize that a 2:1 Ni:Fe molar ratio enhances surface Lewis acidity and hydroxyl density, thereby optimizing tetraethylenepentamine (TEPA) anchoring for robust CO_2 adsorption. From a sensing perspective, we hypothesize that this profound and specific chemisorption will directly translate into an extraordinary mass-loading response, serving as a fundamental proof of concept for highly sensitive gravimetric CO_2 sensors. Simultaneously, *in situ* growth on nickel foam creates a high-surface-area protective layer that increases the number

of catalytic sites for the hydrogen evolution reaction while preventing substrate erosion. The resulting remarkably low charge-transfer resistance makes this LDH-coated NF architecture an extremely promising conductive matrix for future electrochemical sensing. Ultimately, we identify the 2:1 Ni–Fe LDH-coated NF as an optimal candidate for integrated green energy and environmental monitoring technologies.

2. Materials and Methods

2.1 Materials and chemicals

The synthesis precursors included nickel nitrate hexahydrate [$Ni(NO_3)_2 \cdot 6H_2O$, 97%, Katayama Chemical], iron nitrate nonahydrate [$Fe(NO_3)_3 \cdot 9H_2O$, 98%, Daejung], urea [$CO(NH_2)_2$, Katayama Chemical], and ammonium fluoride (NH_4F, 97%, Showa). TEPA (Thermo Scientific) was employed for surface functionalization. NF with a porosity of approximately 95% was used as the conductive substrate. All experimental solutions were prepared using deionized (DI) water.

2.2 Synthesis of Ni–Fe LDHs

Ni-Fe LDHs with various Ni:Fe molar ratios (2:1, 2.5:1, and 3:1) were synthesized via a modified hydrothermal method. For the 2:1 ratio, 1.329 g of nickel nitrate, 0.923 g of iron nitrate, 0.635 g of ammonium fluoride, and 2.059 g of urea were dissolved in 120 g of DI water. The mixture was transferred into a 150 mL Teflon bottle, sealed with 15 wraps of polytetrafluoroethylene (PTFE) tape, and heated in an oven at 120 °C for 12 h. To achieve scalability, multiple Teflon bottles were processed simultaneously in the same oven, increasing the single-batch yield from 4 to 40 g. The resulting precipitates were washed with DI water to pH 7 and dried at 60 °C for 48 h.

2.3 TEPA functionalization and CO_2 adsorption

The LDH samples were surface-modified via a wet impregnation method, where TEPA was dissolved in ethanol at 5–25 wt% relative to the LDH mass. The LDH powder and TEPA–ethanol solution were mixed at a 1:1 mass ratio, stirred at 120 rpm for 10 min, and then dried at 60 °C for 12 h. For adsorption tests, the functionalized powders were placed in a sealed chamber, evacuated, and then exposed to pure CO_2 (99.99%) at ambient pressure for 24 h. CO_2 uptake was quantified via thermogravimetric analysis (TGA) by measuring the weight loss between 100 and 164 °C. The weight loss below 100 °C was mainly attributed to the removal of physically adsorbed and interlayer water, whereas the gradual weight loss above 180 °C was associated primarily with TEPA decomposition and LDH dehydroxylation. Therefore, the weight loss between 100 and 164 °C was assigned mainly to the desorption of CO_2 species chemically bound to the amine groups of TEPA and was used to estimate the CO_2 adsorption capacity.[15]

2.4 Preparation of LDH/NF and alkaline water electrolysis

NF (porosity ~95%, 2 × 3 cm²) was cleaned ultrasonically in acetone and DI water, then placed inside the Teflon bottle during the same hydrothermal process, enabling in situ LDH coating. After rinsing to pH 7 and drying at 60 °C for 48 h, the LDH/NF electrodes were used directly. Alkaline water electrolysis was carried out in 1 M KOH with LDHs/NF as the cathode and a Pt wire as the anode at a constant current of 10 mA. Hydrogen volume was measured from the water displacement using inverted graduated cylinders, and product gas purity was verified by GC. Electrode impedance was measured by EIS (100 kHz–0.01 Hz, 10 mV amplitude, open-circuit potential) before and after testing.

3. Results and Discussion

3.1 Morphology and structural analysis of Ni–Fe LDHs

The morphology and crystal structure of the synthesized Ni–Fe LDH powders were characterized by SEM, TEM, and X-ray diffraction (XRD) to confirm the successful formation of the layered architecture. Figure 1(a) illustrates the surface morphology of the samples, revealing distinct platelet-like structures with an average particle size of approximately 300 nm. These observations confirm that the hydrothermal method provides sufficient autogenous pressure and uniform thermal conditions for the isotropic growth of the layered crystals.

Figure 1(b) shows a TEM image that clearly displays the characteristic layered features. The samples are primarily composed of numerous thin, interlaced nanosheet structures, partially stacked to form a typical layered arrangement. Variations in transparency and overlapping features observed in the TEM image suggest that the individual nanosheets are extremely thin. These sheets represent the positively charged Ni^{2+} and Fe^{3+} metal hydroxide layers, which are charge-balanced by interlayer anions and water molecules, forming a regular two-dimensional structure. This layered architecture is a hallmark of Ni–Fe LDHs and is fundamentally linked to their large accessible interfacial area and ion-exchange capability. The approximately 300 nm lateral dimension, combined with the ultrathin nanosheet morphology, provides abundant exposed surface and edge sites as well as shortened transport pathways. For CO_2 adsorption, the exposed hydroxyl groups on the nanosheet surfaces facilitate TEPA anchoring and improve the accessibility of amine groups for CO_2 chemisorption.[16] For electrochemical applications, the nanosheet architecture increases the contact area between the active material and the electrolyte, exposes more Ni–Fe catalytic sites, and shortens ion- and electron-transport pathways. When grown on nickel foam, the interconnected nanosheets may also facilitate electrolyte penetration and hydrogen-bubble release, thereby contributing to lower interfacial charge-transfer resistance and improved hydrogen-evolution kinetics.

Figure 1(c) displays the XRD patterns of Ni–Fe LDHs synthesized at Ni:Fe molar ratios of 2:1, 2.5:1, and 3:1. All compositions exhibit sharp diffraction peaks with narrow full width at half-maximum (FWHM) values, indicating high crystallinity and a well-defined layered stacking structure. Only slight shifts in peak positions and minor variations in relative intensity

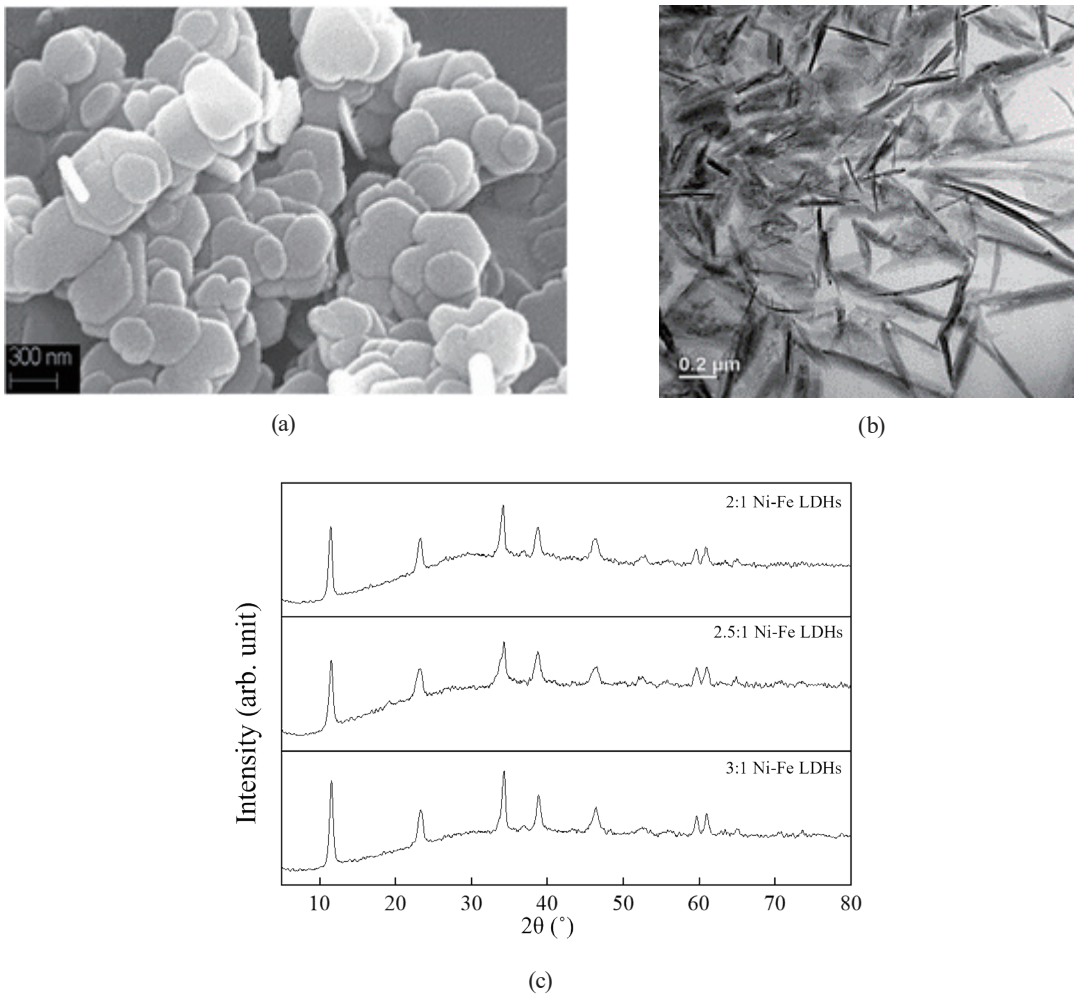


Fig. 1. Characterization of Ni–Fe LDHs: (a) SEM and (b) TEM images, and (c) XRD patterns at various Ni:Fe ratios.

are observed among the different compositions. These subtle differences can be associated with the partial substitution of Ni^{2+} by Fe^{3+} within the brucite-like hydroxide layers. Owing to the slightly smaller ionic radius and higher charge of Fe^{3+} than of Ni^{2+}, variations in Fe content may slightly modify the metal–oxygen bond distances, local lattice distortion, layer charge density, and interlayer electrostatic interactions. Nevertheless, the characteristic LDH diffraction peaks remain at similar positions for all samples, indicating that the compositional variation does not induce a significant phase transformation or disrupt the layered framework. Furthermore, the absence of diffraction peaks corresponding to impurity phases confirms that the hydrothermal conditions consistently yield pure, single-phase Ni–Fe LDHs across the investigated compositional range.

3.2 Effect of TEPA functionalization on CO2 adsorption performance

The qualitative analysis of TEPA functionalization was performed by Fourier transform infrared (FTIR) spectroscopy, as shown in Fig. 2. The N–H stretching and bending bands at approximately 3321 and 1637 cm^{-1}, respectively, reached their highest intensities in the sample containing 20 wt% TEPA. The bands assigned in this study to O–H–related interactions at approximately 2947 and 1357 cm^{-1} also exhibited the strongest signals at this loading, indicating effective interactions and hydrogen bonding between TEPA and the hydroxyl groups on the LDH surface. From a sensor design perspective, this dense and well-anchored array of amine and hydroxyl groups serves as highly specific chemical recognition sites, which are essential for selectively capturing target gas molecules. At lower TEPA loadings, such as 15 wt%, the limited number of amine groups resulted in an insufficient density of active sites for CO_2 chemisorption. Increasing the TEPA content to 20 wt% provided a favorable balance between the density of amine groups and their accessibility to CO_2 molecules.

When the TEPA loading was further increased to 25 wt%, however, excessive TEPA likely accumulated and aggregated on the LDH nanosheets, forming a thicker and less uniformly distributed organic layer. Consequently, some amine groups may have become buried through intermolecular association and hydrogen bonding, while the spaces between adjacent nanosheets and the diffusion pathways for CO_2 molecules may have been partially obstructed. Therefore, although the total TEPA content was higher, the proportion of accessible amine sites available for CO_2 chemisorption decreased. These results indicate 20 wt% TEPA to be the optimal loading among the investigated conditions, because it provided the most favorable balance between active-site density and accessibility.

The quantitative CO_2 adsorption capacity was evaluated by TGA, and the results are shown in Figs. 3(a)–3(d). The weight-loss curves of all samples exhibited three distinct regions. The weight loss from 30 to 100 °C was mainly attributed to the removal of physically adsorbed and interlayer water. The subsequent weight loss from 100 to 164 °C was assigned to the primary

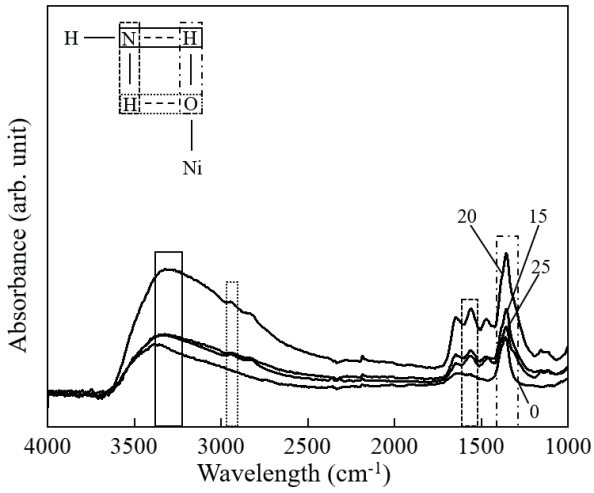


Fig. 2. FTIR spectra and hydrogen bonding mechanism of TEPA-functionalized Ni–Fe LDHs.

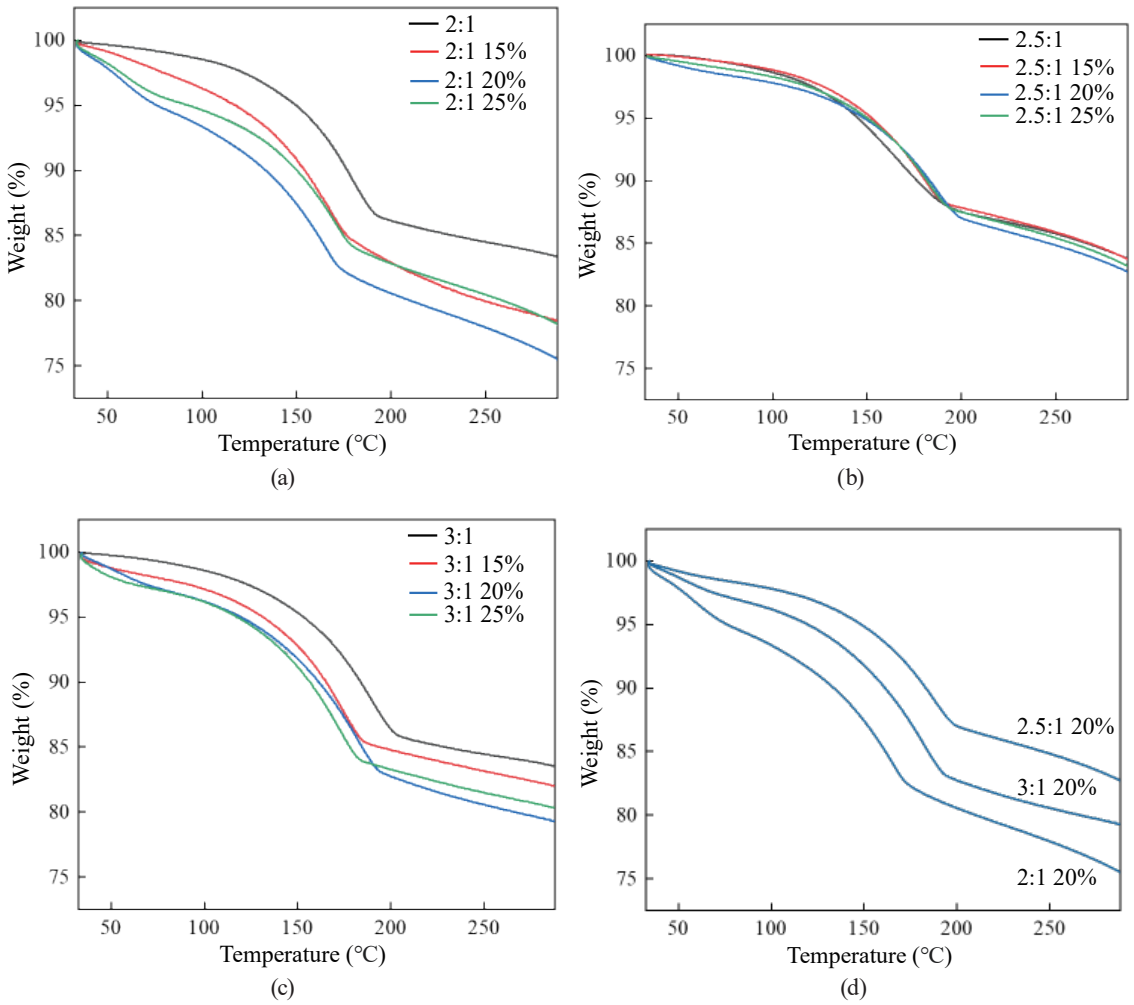


Fig. 3. (Color online) TGA curves of (a)–(c) Ni–Fe LDHs with various TEPA loadings and (d) comparison of different Ni:Fe ratios at 20 wt%.

desorption of chemically adsorbed CO_2, whereas the gradual weight loss above 180 °C was associated with TEPA decomposition and LDH dehydroxylation. Consistent with the FTIR results, the samples containing 20 wt% TEPA exhibited the highest CO_2 uptake among the investigated TEPA loadings. Among the different compositions, the Ni–Fe LDHs with a Ni:Fe molar ratio of 2:1 achieved the highest CO_2 uptake of 0.389 g CO_2/g at a TEPA loading of 20 wt%, exceeding those of the 2.5:1 and 3:1 samples, which exhibited adsorption capacities of 0.314 and 0.251 g CO_2/g, respectively. This improved performance may be associated with the higher Fe^{3+} fraction in the 2:1 composition. The incorporation of Fe^{3+} increases the positive charge density of the LDH hydroxide layers and modifies the local Lewis acidity and surface hydroxyl environment. These Fe^{3+}-associated surface sites can strengthen the interaction of TEPA with LDHs through coordination and hydrogen bonding, thereby improving TEPA anchoring and reducing the loss or aggregation of amine molecules. As a result, a greater proportion of primary and secondary amine groups remains accessible for reaction with CO_2. These accessible amine sites subsequently react with CO_2 to form chemically adsorbed amine–

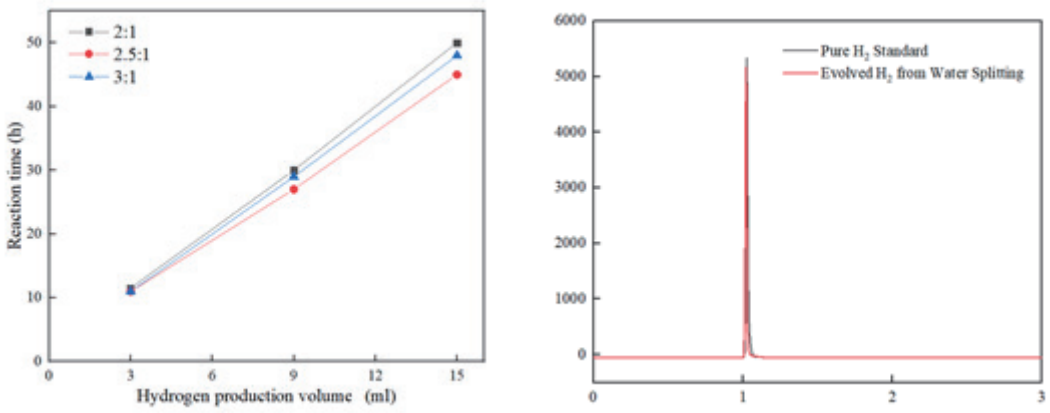
CO_2 species, thereby enhancing the overall CO_2 uptake. Therefore, Fe^{3+} does not primarily adsorb CO_2 directly; instead, it promotes CO_2 chemisorption by stabilizing TEPA and increasing the availability of reactive amine sites.

The adsorption capacity of the 2:1 Ni–Fe LDH/TEPA sample is also higher than the values typically reported for amine-functionalized solid adsorbents, which generally range from 0.09 to 0.26 g CO_2/g.[17] From a gravimetric sensing perspective, the adsorption of CO_2 increases the mass of the recognition layer. When such a material is integrated with a mass-sensitive transducer, such as a quartz crystal microbalance, surface acoustic wave device, or microresonator, the adsorption-induced mass change can be converted into a measurable frequency shift. Under otherwise identical sensing conditions, a larger amount of adsorbed CO_2 may produce a greater mass change and, consequently, a larger gravimetric response. Therefore, the relatively high CO_2 uptake of the 2:1 Ni–Fe LDH/TEPA sample indicates its potential to generate a detectable mass-loading signal. However, the equilibrium adsorption capacity measured by TGA is not directly equivalent to sensor sensitivity or dynamic sensor response. Practical sensing performance also depends on the CO_2 concentration, sensing-layer thickness and mass, adsorption and desorption kinetics, transducer characteristics, humidity interference, selectivity, reversibility, detection limit, and cycling stability. Accordingly, the present adsorption results demonstrate the potential of this material as a gravimetric CO_2 recognition layer, rather than confirming the performance of a complete CO_2 sensor. Further device-level measurements are required to validate its sensing capability.

3.3 Alkaline water electrolysis: Catalytic activity and durability testing

The electrocatalytic performance was evaluated in 1 M KOH at a constant current of 10 mA. Ni–Fe LDH-coated nickel foam with a Ni:Fe molar ratio of 2:1 exhibited the highest activity and durability, yielding 30 mL of H_2 after 9 h (an 11% improvement compared with bare NF) and a total of 50 mL over 15 h, as shown in Fig. 4(a). While bare NF corroded and failed after 9 h, the LDH coating provided an additional catalytic interface and protected the nickel foam from surface oxidation and passivation during prolonged electrolysis. Gas chromatography confirmed high-purity hydrogen production, with a peak at 1.0 min matching the hydrogen standard, as shown in Fig. 4(b).

The superior hydrogen production of the 2:1 composition may be associated with its higher Fe^{3+} content and the synergistic interaction between Ni and Fe sites. In alkaline media, the hydrogen evolution reaction begins with water dissociation through the Volmer step, in which H_2O accepts an electron to form an adsorbed hydrogen intermediate (H) and OH^-.[18] Previous studies have revealed that Fe incorporation can modify the local electronic structure of NiFe-based catalysts and facilitate water adsorption and O–H bond cleavage. Therefore, the higher Fe^{3+} fraction in the 2:1 composition may increase the relative abundance of Ni–O–Fe cooperative environments, while adjacent Ni-containing sites participate in the adsorption and subsequent conversion of H into H_2. Accordingly, the 2:1 composition may provide a more favorable balance among water dissociation, hydrogen-intermediate conversion, and interfacial electron transfer than the 2.5:1 and 3:1 compositions. Electrochemical impedance spectroscopy further verified



(a) (b)

Fig. 4. (Color online) (a) H2 evolution profiles and (b) GC analysis for gas purity verification of Ni–Fe LDH-coated electrodes.

that the 2:1 electrode maintained the lowest charge-transfer resistance, demonstrating faster interfacial charge transport and more favorable hydrogen-evolution kinetics, as shown in Fig. 5.

Furthermore, the interfacial charge-transfer behavior of the electrodes was evaluated using EIS Nyquist plots, as shown in Fig. 5. Under comparable measurement conditions, a smaller semicircle generally indicates a lower charge-transfer resistance (Rct) and more rapid electron transfer across the electrode–electrolyte interface. For bare NF, the semicircle diameter increased markedly with electrolysis time, suggesting the progressive deterioration of the interfacial charge-transfer kinetics. This behavior may be attributed to surface oxidation and the formation of a passivation layer, which obstruct electron transfer and reduce the number of accessible reaction sites, as shown in Fig. 5(a). In contrast, the LDH-coated electrodes generally exhibited more favorable interfacial charge-transfer behavior, as shown in Figs. 5(b)–5(d).

Among the investigated compositions, the Ni–Fe LDH-coated NF with a Ni:Fe molar ratio of 2:1 exhibited the smallest Nyquist semicircle before and after electrolysis, as shown in Fig. 5(c). This result qualitatively indicates that the 2:1 electrode exhibited the lowest interfacial charge-transfer resistance and maintained the most favorable charge-transport behavior during prolonged operation. The reduced resistance facilitates electron transfer from the nickel-foam substrate to the Ni–Fe catalytic sites, thereby supporting water dissociation and the formation and conversion of adsorbed hydrogen intermediates during the alkaline hydrogen evolution reaction. Under the constant-current conditions used in this study, the lower interfacial resistance does not increase the applied current; instead, it reduces polarization and charge-transfer losses, and enables the supplied charge to participate more effectively in hydrogen evolution.

In comparison, the 2.5:1 and 3:1 electrodes exhibited larger Nyquist semicircles, indicating slower interfacial charge-transfer kinetics. This trend is consistent with their slightly lower accumulated hydrogen volumes. The combined hydrogen-production and EIS results therefore suggest that the superior performance of the 2:1 electrode arises from the combined effects of favorable Ni–Fe cooperative sites, enhanced alkaline water-dissociation kinetics, lower interfacial charge-transfer resistance, and the suppression of nickel-foam passivation.

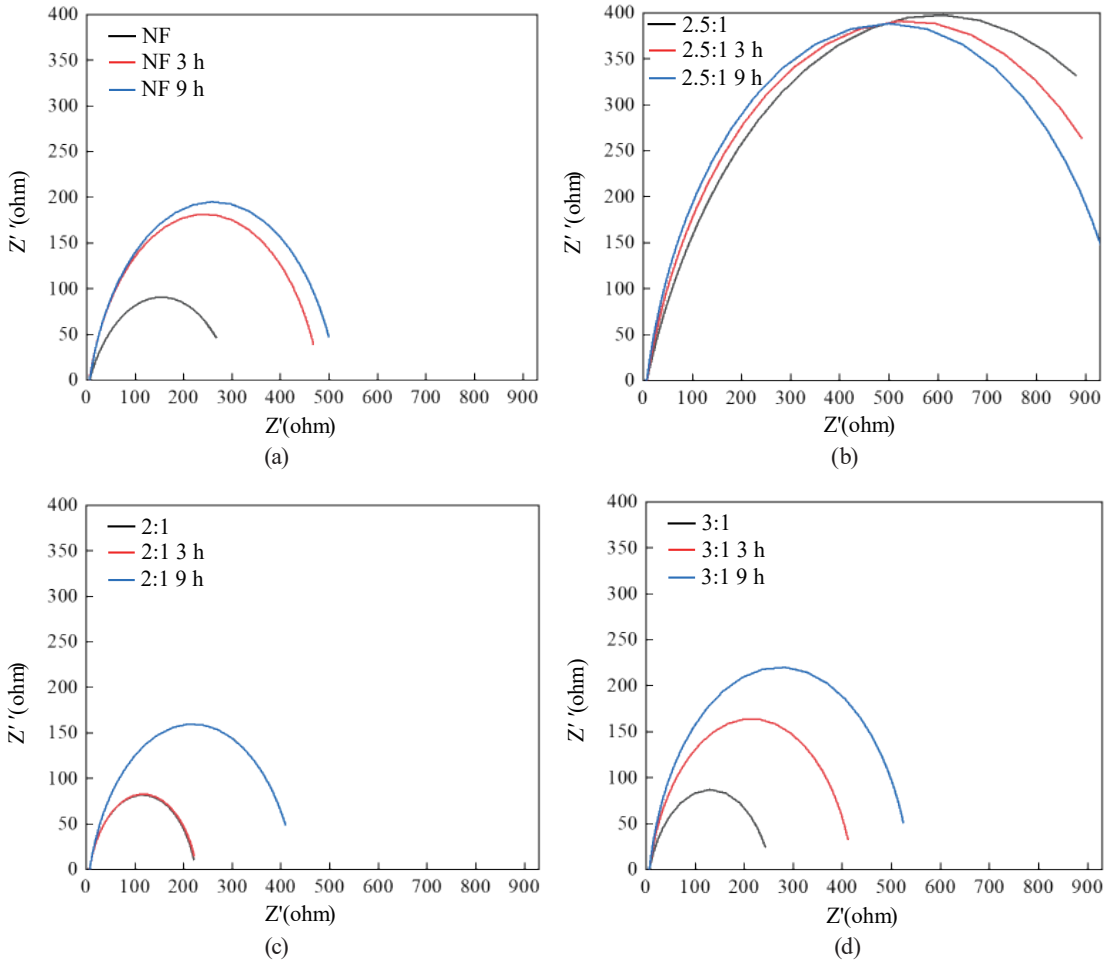


Fig. 5. (Color online) EIS Nyquist plots of (a) NF and Ni–Fe LDHs with molar ratios of (b) 2.5:1, (c) 2:1, and (d) 3:1.

Consequently, the 2:1 composition exhibited the highest hydrogen production and electrochemical durability among the investigated electrodes.

4. Conclusions

In this study, we systematically developed Ni–Fe LDHs with various molar ratios of 2:1, 2.5:1, and 3:1. The results successfully validated their superior performance in carbon dioxide capture and alkaline water electrolysis. SEM, TEM, and XRD analyses confirmed that the synthesized LDHs possess a highly ordered two-dimensional layered structure with excellent crystallinity. The materials exhibit an average particle size of approximately 300 nm, providing ample surface active sites for subsequent reactions.

In carbon dioxide adsorption applications, a TEPA loading of 20 wt% was found to achieve the optimal balance between active site density and pore accessibility. Among all compositions, the sample with a Ni:Fe ratio of 2:1 exhibited the highest carbon dioxide uptake of 0.389 g CO_2/g. This significantly outperformed the samples with 2.5:1 (0.314 g CO_2/g) and 3:1 (0.251 g CO_2/g)

ratios. This performance advantage is attributed to the higher Fe^{3+} content, which provides stronger Lewis acidity and higher surface hydroxyl density to effectively anchor TEPA molecules and promote robust CO_2 chemisorption. Crucially, this extraordinary capture capacity translates into a massive mass-loading response, demonstrating its immense potential as an ultrasensitive recognition layer for gravimetric CO_2 gas sensors.

In alkaline water electrolysis, the *in situ* coating of LDHs on NF electrodes markedly enhanced both catalytic activity and corrosion resistance. The Ni–Fe LDH-coated NF with a Ni:Fe molar ratio of 2:1 delivered the highest performance at a constant current of 10 mA. It produced 30 mL of hydrogen after 9 h, representing approximately an 11% improvement over bare NF. Furthermore, the electrode maintained stable operation for up to 15 h, yielding a total of 50 mL. Gas chromatography confirmed that the produced gas was high-purity hydrogen. Electrochemical impedance spectroscopy further confirmed that the Ni–Fe LDH-coated NF with a Ni:Fe molar ratio of 2:1 maintains the lowest charge-transfer resistance, demonstrating superior charge-transport kinetics. Beyond clean energy production, such excellent interfacial stability and rapid electron transfer make this robust architecture a highly promising conductive matrix for advanced electrochemical sensing platforms.

Overall, the results identify the Ni:Fe molar ratio of 2:1 as the optimal chemical composition for integrated applications in carbon capture and clean hydrogen production. This study establishes a solid foundation for the future engineering development of green energy technologies.

Acknowledgments

This work was supported by the National Science and Technology Council (NSTC), Taiwan, under Grants No.112-2221-E-006-173, 113-2221-E-006-087-MY2, 113-2221-E-006-112-MY2, and 113-2221-E-006-116. The authors gratefully acknowledge the Core Facility Center at National Cheng Kung University, Taiwan, for providing access to the EM000800 and SQUID000200 instruments, which were funded by the NSTC project 114-2740-M-006-001. Additional support from the Higher Education Sprout Project of the Ministry of Education, Taiwan, through the Headquarters of University Advancement at National Cheng Kung University (NCKU), is also gratefully acknowledged.

References

1 H. McLaughlin, A. A. Littlefield, M. Menefee, A. Kinzer, T. Hull, B. K. Sovacool, M. D. Bazilian, J. Kim, and S. Griffiths: Renewable Sustainable Energy Rev. **177** (2023) 113215.
2 H. Tüysüz: Acc. Chem. Res. **57** (2024) 558. https://doi.org/10.1021/acs.accounts.3c00709
3 G. Zhang, P. Zhao, Y. Xu, Z. Yang, H. Cheng, and Y. Zhang: ACS Appl. Mater. Iinterfaces **10** (2018) 34340.
4 Z. Gu, X. Wang, P. Huang, Y. Huang, X. He, X. Wei, J. Yue, J. Jiang, and C. Zhao: Process Saf. Environ. Prot. **160** (2022) 573. https://doi.org/10.1016/j.psep.2022.02.047.
5 S. Zhao, Y. Zhang, L. Li, J. Feng, W. Qiu, Y. Ning, Z. Huang, and H. Lin: Sep. Purif. Technol. **354** (2025) 129586. https://doi.org/10.1016/j.seppur.2024.129586
6 L. Tan, J. Yu, C. Wang, H. Wang, X. Liu, H. Gao, L. Xin, D. Liu, W. Hou, and T. Zhan: Adv. Funct. Mater. **32** (2022) 2200951. https://doi.org/10.1002/adfm.202200951
7 K. Siwek, S. Eugénio, D. Santos, M. Silva, and M. Montemor: Int. J. Hydrogen Energy **44** (2019) 1701. https://doi.org/10.1016/j.ijhydene.2018.11.070

8 L. Li, B. Wang, G. Zhang, G. Yang, T. Yang, S. Yang, and S. Yang: Adv. Energy Mater. **10** (2020) 2001600. https://doi.org/10.1002/aenm.202001600
9 D. Bhalothia, A. Beniwal, H. Gurjar, K. Shekhawat, A. Bagaria, and T. Y. Chen: Small **21** (2025) e06018. https://doi.org/10.1002/smll.202506018
10 H.-M. Deng, G.-Y. Chen, and S.-C. Shi: Sens. Mater. **38** (2026) 3007. https://doi.org/10.18494/SAM5964
11 D. Rahmadiawan, H. Abral, S. Shih-Chen, T.-T. Huang, R. Zainul, and H. Nurdin: Tribol. Ind. **45** (2023) 367. http://dx.doi.org/10.24874/ti.1482.05.23.06
12 S.-C. Shi, X.-N. Tsai, and D. Rahmadiawan: Surf. Coat. Technol. **483** (2024) 130712. https://doi.org/10.1016/j.surfcoat.2024.130712
13 A. Seijas-Da Silva, A. Hartert, V. Oestreicher, J. Romero, C. Jaramillo-Hernández, L. J. Muris, G. Thorez, B. J. Vieira, G. Ducourthial, and A. Fiocco: Nat. Commun. **16** (2025) 6138. https://doi.org/10.1038/s41467-025-61356-2
14 G. Wang, X. Wang, R. Li, C. Yu, and T. Zhen: Catalysts **15** (2025) 111. https://doi.org/10.3390/catal15020111
15 N. Thouchprasitchai, N. Pintuyothin, and S. Pongstabodee: J. Environ. Sci. **65** (2018) 293. http://dx.doi.org/10.1016/j.jes.2017.02.015
16 B. Ge, C. Chen, Z. Gan, X. Zhu, Y. Miao, Y. Wang, T. Ge, D. O'Hare, and R. Wang: ACS Sustainable Chem. Eng. **11** (2023) 9282. https://doi.org/10.1021/acssuschemeng.3c01183
17 R. Girimonte, F. Testa, M. Turano, G. Leone, M. Gallo, and G. Golemme: Processes **10** (2022) 422. https://doi.org/10.3390/pr10020422
18 W. Li, Z. Ni, O. Akdim, T. Liu, B. Zhu, P. Kuang, and J. Yu: Adv. Mater. **37** (2025) 2503742. https://doi.org/10.1002/adma.202503742